that are losing their tritium by exchange through the formation of the enamine phosphate. Unfortunately, no data are at present available on the rate of this exchange and, thus, on the actual concentration of the enamine phosphate intermediate.

(3) At −24 °C and pH* 5.24, the amount of hexose bisphosphate formed by reaction of the aldolase–dihydroxyacetone phosphate complex with DL-glyceraldehyde 3-phosphate is larger than the amount of the acid-labile species consumed, thus showing that an additional species, besides the acid-labile one, is trapped by DL-glyceraldehyde 3-phosphate. This species cannot be represented by the molecules of the substrate free in the medium since no exchange was detected in the course of the experiment between dihydroxy[^{14}C]acetone phosphate of the medium and the unlabeled dihydroxyacetone phosphate bound to the enzyme. The additional trapping species are thus the other enzyme–substrate intermediates, including the enamine phosphate that is directly involved in the trapping.

Registry No. Fructose-1,6-bisphosphate aldolase, 9024-52-6; dihydroxyacetone phosphate, 57-04-5.

References

Baranowski, T., & Niederland, T. R. (1949) *J. Biol. Chem. 180*, 543–548.
Bradford, M. M. (1976) *Anal. Biochem. 72*, 248–254.
Bray, G. A. (1960) *Anal. Biochem. 1*, 279–285.
Crowden, A. L., III, Barker, R., & Swenson, C. A. (1973) *Biochemistry 12*, 2078–2083.
Donovan, J. W. (1969) *J. Biol. Chem. 244*, 1961–1967.
Ginsburg, A., & Mehler, A. H. (1966) *Biochemistry 5*, 2623–2634.
Grazi, E., & Trombetta, G. (1978) *Biochem. J. 175*, 361–365.
Grazi, E., & Trombetta, G. (1979) *Eur. J. Biochem. 100*, 197–202.
Grazi, E., & Trombetta, G. (1980) *Arch. Biochem. Biophys. 200*, 31–39.
Grazi, E., Trombetta, G., & Lanzara, V. (1983) *Biochem. Biophys. Res. Commun. 110*, 578–583.
Iyengar, R., & Rose, I. A. (1981) *Biochemistry 20*, 1223–1229.
Kawahara, K., & Tanford, C. (1966) *Biochemistry 5*, 1578–1584.
Kokesh, F. C., & Kakuda, Y. (1977) *Biochemistry 16*, 2467–2473.
Larroque, C., Maurel, P., Calny, C., & Douzou, P. (1976) *Anal. Biochem. 73*, 9–19.
Racker, E. (1947) *J. Biol. Chem. 167*, 842–852.
Rose, I. A., & Rieder, S. V. (1955) *J. Am. Chem. Soc. 77*, 5764–5769.
Tashima, Y., & Yoshimura, N. (1975) *J. Biochem. (Tokyo) 78*, 1161–1169.

Applicability of the Induced-Fit Model to Glyceraldehyde-3-phosphate Dehydrogenase from Sturgeon Muscle. Study of the Binding of Oxidized Nicotinamide Adenine Dinucleotide and Nicotinamide 8-Bromoadenine Dinucleotide†

Guy Branlant,* Brigitte Eiler, Jean-François Biellmann, Hans-Peter Lutz, and Pier Luigi Luisi

ABSTRACT: A new method of calculation, based on a direct fitting of the protein fluorescence intensity observed upon coenzyme binding (H.-P. Lutz, unpublished results), is used to study the negative cooperative behavior of glyceraldehyde-3-phosphate dehydrogenase from sturgeon muscle. The calculation procedure simultaneously elaborates data obtained for four different protein concentrations, and it is able to compare different models by computing the minimal and critical sum of squares. Using this approach, it is shown that the induced-fit model [Koshland, D. E., Jr., Nemethy, G., & Filmer, D. (1966) *Biochemistry 5*, 365] and the dimer of dimer model [Malhotra, O. P., & Bernhard, S. A. (1968) *J. Biol. Chem. 243*, 1243–1252] can both be applied for explaining the negative cooperativity observed upon coenzyme binding to sturgeon glyceraldehyde-3-phosphate dehydrogenase. In addition to the progressive modification of the binding affinity during ligand binding, different maximal fluorescence quenchings for the binding steps must be postulated; and furthermore, the binding capability decreases by decreasing the protein concentration. The fact that the induced-fit model can also be applied is rather in contradiction with the view generally accepted of a dimer of dimer structure of sturgeon glyceraldehyde-3-phosphate dehydrogenase. By use of the same approach, nicotinamide 8-bromoadenine dinucleotide is shown to bind to glyceraldehyde-3-phosphate dehydrogenase from sturgeon in a negative cooperative manner.

Monod et al. (1965) have proposed a model that explains the positive cooperativity of ligand binding to oligomeric proteins. On the other hand, Koshland et al. (1966) have introduced the "induced-fit" model, which explains both positive and negative cooperativity. Both models assume complete symmetry of the nonligated and fully ligated states but differ in so far as the intermediate states are not symmetric in the induced-fit model. Negative cooperativity in ligand binding has been also interpretated by Malhotra & Bernhard (1968) and MacQuarrie & Bernhard (1971) on the basis of preexisting asymmetry in the protein oligomer. In such a case, it is assumed that dimers or tetramers are never symmetric

† From the Laboratoire de Chimie Organique Biologique, Associé au CNRS, Institut de Chimie, Université Louis Pasteur, 67008 Strasbourg, Cedex, France (G.B., B.E., and J.-F.B.), and the Laboratorium für Technische Chemie, Eidgenössische Technische Hochschule, Zürich, Switzerland (H.-P.L. and P.L.L.). *Received December 17, 1982.* This work was supported by a short-term EMBO fellowship.

0006-2960/83/0422-4437$01.50/0

and possess two different classes of binding sites.

Many of the concepts about negative cooperativity of proteins have derived from studies on D-glyceraldehyde-3-phosphate dehydrogenase. Every glyceraldehyde-3-phosphate dehydrogenase isolated either from muscle (Conway & Koshland, 1968; Trentham, 1968; Seydoux et al., 1973) or from *Bacillus stearothermophilus* (Allen & Harris, 1975) exhibits negative cooperativity in binding the coenzyme NAD^+.[1] From the X-ray crystallographic data, it is difficult to discriminate between the model of Bernhard and his colleagues and that proposed by Koshland and co-workers. The interpretation of crystallographic data obtained on the lobster enzyme by Moras et al. (1975) supported the first model. In contrast, the crystallographic data obtained by Biesecker & Wonacott (1977) and Biesecker et al. (1977) did not reveal any asymmetry in the apo- and holoenzyme. Moreover, these authors have shown that significant conformational changes occurring on NAD^+ binding to the tetramer were not restricted only to the binding of the first molecule of NAD^+. Such results are rather in favor of the induced-fit model proposed by Koshland [see also Henis & Levitzki (1980a,b)].

The mechanism of the negative cooperativity, observed in coenzyme binding to glyceraldehyde-3-phosphate dehydrogenase, remains to be explained on molecular terms. The recent studies of Henis & Levitzki (1980a,b) and Branlant et al. (1982) support the idea that the negative cooperativity observed in NAD^+ binding might be triggered by the interactions between the active site and the pyridinium moiety of the coenzyme. On the other hand, the studies of Moras et al. (1975) and Olsen et al. (1976), showing a different binding of the adenine part of NAD^+ and Nbr^8AD^+, are rather suggestive of a preeminent participation of the adenine part in the negative cooperativity phenomenon [see also Levitzki (1974)].

In this paper, we report the results of binding studies of NAD^+ and Nbr^8AD^+ on glyceraldehyde-3-phosphate dehydrogenase from sturgeon muscle. For our binding studies, we used the quenching of the protein fluorescence to measure the binding saturation. To determine this binding saturation and the free-ligand concentration, a new method of calculation based on a direct fitting of the fluorescence intensity observed for several total-ligand concentrations and different protein concentrations (H.-P. Lutz, unpublished results) was used.

Materials and Methods

Materials

The procedure of Seydoux et al. (1973) for purification of glyceraldehyde-3-phosphate dehydrogenase from sturgeon muscle was modified as follows. After ammonium sulfate fractionation, the protein solution (70 mL, i.e., 100 g of sturgeon muscle) was dialyzed against 5 mM EDTA/1 mM DTT, pH 6.6. The solution was then applied to a column of CM-cellulose (CM-52, Whatman column, 2 × 20 cm), equilibrated with 5 mM EDTA, pH 6.6. The enzyme was then eluted with a linear salt gradient of 0–0.2 M KCl in 5 mM EDTA, pH 6.6 (200 mL twice). After dialysis against saturated ammonium sulfate solution adjusted to pH 7, the precipitated enzyme was dissolved in 10 mM Tes, pH 7, 5 mM EDTA, and 1 mM DTT and then dialyzed against the same buffer (final concentration of apoenzyme 20–40 mg/mL, sp act. 330 IU/mg, UV ratio 280/260 = 2.10). As checked by amino acid analysis, this apoenzyme has a composition similar to that published (Allison & Kaplan, 1964). The apoenzyme concentration was determined with an extinction coefficient of 0.895/mg of protein at 280 nm (Seydoux et al., 1973). All the fluorescent measurements were done with freshly prepared apoenzyme. After each experiment, the enzymic activity was measured in order to check the stability of the enzyme. Nbr^8AD^+ was prepared according to a published procedure (Abdallah et al., 1975). Its purity was checked by chromatography on cellulose sheet (Polygram CEL 400) developed by a mixture of isobutyric acid/H_2O/NH_4OH (66/33/1). NAD^+ (grade 1, Boehringer, Germany) was purified by chromatography on QAE-Sephadex A-25 (gradient 50–500 mM sodium chloride). After removal of salt by filtration on a Bio-Gel P-2 column, NAD^+ was judged pure as checked by its chromatographic behavior on cellulose sheet. The concentrations of Nbr^8AD^+ and NAD^+ were calculated by using $\epsilon_{264} = 19 \times 10^3\ M^{-1}\ cm^{-1}$ (Abdallah et al., 1975) and $\epsilon_{258} = 20 \times 10^3\ M^{-1}\ cm^{-1}$, respectively.

Methods

Computation Methods. The binding constants were computed with the program BINDFIT of H.-P. Lutz (unpublished results), which uses for the regression directly the observed fluorescence intensity as a dependent variable and the total ligand and protein concentrations as independent variables. This program works simultaneously with several data series obtained with different protein concentrations, which brings about more accurate results. The activity (binding capability) is fitted independently for each protein concentration (this is to take into account possible activity changes, particularly at low protein concentrations, where the activity cannot be measured by titration under these conditions). Also, nonidentical maximal quenching for each ligand binding step can be introduced as a free parameter. Notice that this does not necessary mean that the four subunits have different fluorescence properties to start with (although it might be so). The program uses the following equations:

$$K_i = \frac{i}{n - i + 1} K'_i \tag{1}$$

$$Y_i = \frac{\prod_{j=1}^{i} L/K_j}{1 + \sum_{k=1}^{n} \prod_{j=1}^{k} L/K_j} \tag{2}$$

$$y = \sum_{i=1}^{n} \frac{i}{n} Y_i \tag{3}$$

$$L = L_{tot} - Y\text{act}B_{tot} \tag{4}$$

$$\Delta f = \sum_{i=1}^{n} (\Delta f_{max,i} \sum_{j=1}^{n} Y_j)\text{act}/n \tag{5}$$

$$F = F_0(1 - \Delta f) \tag{6}$$

where act is activity (binding capability), i.e., the fraction of sites that can bind a ligand (function of B_{tot}), B_{tot} is total binding site concentration ("normality"), F is fluorescence intensity, F_0 is fluorescence intensity for the protein without ligand bound, Δf is relative quenching (relative to F_0), $\Delta f_{max,i}$ is maximal relative quenching for the ith ligand binding step for the fully active protein, K_i is the global (macroscopic) dissociation constant for the ith ligand binding step, K'_i is the

[1] Abbreviations: NAD^+, oxidized nicotinamide adenine dinucleotide; Tes, 2-[[tris(hydroxymethyl)methyl]amino]ethanesulfonic acid; DTT, dithiothreitol; Nbr^8AD^+, nicotinamide 8-bromoadenine dinucleotide; KNF model, Koshland–Nemethy–Filmer model; PEA model, preexistent asymmetry model of Bernhard and co-workers; ϵNAD^+, nicotinamide 1,N^6-ethenoadenine dinucleotide; EDTA, ethylenediaminetetraacetic acid.

intrinsic (microscopic) dissociation constant, L is free ligand concentration, L_{tot} is total ligand concentration, n is number of sites per protein, Y_i is fraction of active protein with i ligands bound, and y is binding saturation (fraction of saturated active binding sites).

Equations 1 and 2 inserted in eq 3 (the Adair equation [see Adair (1925)] and combined with eq 4 lead to a system from which L can be calculated iteratively from L_{tot} and B_{tot} with K'_i and act given as parameters. Y_i can now be calculated from L with eq 2 and 5; F is obtained as a function of L_{tot} and B_{tot} with K'_i, act, and $\Delta f_{max,i}$ given as parameters. The sum of squared differences between this calculated F and the observed intensities is used in this program for the regression on the parameters (nonlinear least-squares fit). The most general case that can be treated with these equations is the case of a protein having independent binding constants and nonidentical maximal quenchings for the different ligand binding steps and nonidentical activities for different protein concentrations. This general model can be easily transformed into particular models, e.g., one in which the maximal quenching for the different binding steps and/or the activities for the different protein concentrations are equal and/or one in which constraints to the binding constants according to models in literature (Table I) are introduced. The validity of each particular model can be tested by comparing the minimal sum of squares with the critical one computed for the most general case. This critical sum of squares gives the confidence limit for the sum of squares of a set of values for the parameters and is calculated with the established statistical F test (Draper & Smith, 1966) for 95% confidence level in this program. In particular, all those models resulting in a minimal sum of squares smaller than the critical one for the most general case lie inside the confidence limits. Out of those models that fit the data accurately, the model with the least number of free parameters will be prefered.

Summarizing the main advantages of our procedure in comparison with the traditional computational methods, we note the following: (i) Linearization for the Hill or Scatchard plots lead to errors because of the wrong weighting of the experimental errors (especially, the Scatchard plot shows a great sensitivity to errors in the low saturation region). For this reason, our program features a regresssion performed on the variables that are directly measured (e.g., fluorescence as a function of ligand concentration instead of mathematically transformed values of these quantities) and is more accurate. (ii) The transformation of fluorescence intensities into binding saturation values requires a very precise estimation of the maximal quenching, Δf_{max}. This is not necessary with this program, because Δf_{max} is introduced as a parameter. (iii) The determination of the activity (binding capability) is generally not possible at low protein concentrations. A change of activity with the protein concentration can be taken into account by using the activity as a parameter, as is done here. (iv) In our program the total ligand concentration is used as the independent variable instead of the free-ligand concentration (as is usual in the Adair equation). Generally, the free-ligand concentration is calculated (if not directly measured) from the total-ligand concentration and from the binding saturation, but this introduces the experimental errors of fluorescence measurements into the independent variable (which affects the statistical analysis). (v) The program permits analysis of data with a model having nonidentical maximal quenchings for each ligand binding step. This can be performed, as in the present program, by direct fitting of the fluorescence intensity data. (vi) The present procedure numerically evaluates whether a proposed model is within or outside the confidence contour of the most general model.

Table I: Constraints for Intrinsic Dissociation Constants in Adair Equation Leading to Different Binding Models for Tetrameric Proteins (Cornish-Bowden & Koshland, 1970)

model	relationship of intrinsic dissociation constants
identical binding sites with no interaction	$K'_1 = K'_2 = K'_3 = K'_4$
two kinds of binding sites (PEA)	leads to a dimer model
simple KNF models	
square	$^1/_3 < K'_1/K'_2 = K'_3/K'_4 > K'_2/K'_3$
tetrahedral	$K'_1/K'_2 = K'_2/K'_3 = K'_3/K'_4$

Spectrofluorometric Measurements. The fluorescence was measured with an Aminco SPF-1000 fluorometer with a thermostated cell holder and a cell shift compartment for inner filter effect correction (H.-P. Lutz and P. L. Luisi, unpublished results). The excitation of the enzyme fluorescence was at 290 nm, and the emission was observed at 340 nm. The fluorescence intensity was recorded with a papertape puncher connected to a digital voltmeter. The measurements with glyceraldehyde-3-phosphate dehydrogenase and the ligands NAD^+ and Nbr^8AD^+ were performed at a temperature of 18 °C with four different protein concentrations (0.1, 0.3, 1.0, and 3.5 μM in binding sites) in 10 mM Tes buffer, pH 7, 5 mM EDTA, and 1 mM DTT. Fluorescence intensity (F_0) was measured for the pure protein solution. Ligand stock solution was then added successively until the ligand concentration was about 10 times the binding site concentration (in order to avoid dilution of the protein and the consequent experimental errors, the coenzyme stock solution also contained protein in the same concentration as the sample solution). The rough data were treated by the program DBIND running on a pdp-8/e computer that corrected for inner filter effects and computed the total-ligand concentration (corrected for the increases of volume from addition of ligand solution).

Results

As visualized in the Scatchard plot representation (Figure 1), NAD^+ and Nbr^8AD^+ bind to glyceraldehyde-3-phosphate dehydrogenase from sturgeon in a negative cooperative manner. Regression analysis was performed according to the procedure described above and by assuming different models for ligand binding. The models used and the corresponding constraints on the intrinsic binding constants are listed in Table I. Also, the models assuming equal activities for different protein concentrations and equal maximal quenchings were tried. Results are shown in Table II in terms of sums of squares and microscopic binding constants. Also, the number of free parameters elaborated by the computer program is given. As indicated under Materials and Methods, the main criterium for evaluating the model validity is to compare the critical sum of squares of the most general model with the minimal sum of squares of each model. Table II shows clearly that the binding model has to assume that the activity changes for the different protein concentrations and that there must be different maximal quenchings for the four ligand binding steps (introducing equal activities or equal quenching leads to significantly worse sum of squares). One can also exclude the case of equal sites with no interaction. In the case of NAD^+, this is visualized in the primary plots (Figure 2). These plots show that the dimer of dimer model and the tetrahedral KNF model, with nonidentical activities and maximal quenchings for both models, fit the experimental data

Table II: Best Fitting Parameters for Different Models[a]

constraints	sum of squares: minimal	sum of squares: critical	K'_1 (μM)	K'_2 (μM)	K'_3 (μM)	K'_4 (μM)	no. of free parameters
Glyceraldehyde-3-phosphate Dehydrogenase + NAD^+							
no constraints	939.0	1125.0	0.064	0.211	0.126	0.361	12
equal quenching	1632.0		0.036	0.125	0.205	0.524	9
equal quenching and equal activities	2612.0		0.079	0.136	0.238	0.665	8
tetrahedral KNF model	997.0	1164.0	0.093	0.163	0.286	0.504	10
dimer of dimers	1513.0		0.092	0.449			8
equal sites with no interactions	2273.0		0.132	0.132	0.132	0.132	9
Glyceraldehyde-3-phosphate Dehydrogenase + Nbr^8AD^+							
no constraints	1121.0	1345.0	0.048	0.250	0.205	0.526	12
equal quenching	2067.0		0.016	0.105	0.174	0.531	9
equal quenching and equal activities	6059.0		0.037	0.126	0.246	0.508	6
tetrahedral KNF model	1238.0	1446.0	0.072	0.151	0.315	0.657	10
dimer of dimers	1948.0		0.070	0.436			8
equal sites with no interactions	4124.0		0.115	0.115	0.115	0.115	9

[a] No constraints means independent binding constants in the Adair equation, nonidentical activities for different protein concentrations, and nonequal efficiency quenchings for the different ligand binding steps. Equal activities means that the binding efficiency does not vary with protein concentration.

Table III: Best Fitting Parameters for Tetrahedral KNF Model

	ligand binding step: 1	2	3	4	B_{tot} (μM)	act.[a]	act.[b]
			NAD^+				
K'_i (μM)	0.09	0.16	0.29	0.50	0.082	0.73	0.68
					0.281	0.93	0.87
$\Delta f_{max,i}$	0.88	0.56	0.57	0.40	0.980	0.94	0.87
					3.57	0.98	0.90
			Nbr^8AD^+				
K'_i (μM)	0.07	0.15	0.31	0.66	0.082	0.78	
					0.282	0.97	
$\Delta f_{max,i}$	0.90	0.59	0.55	0.36	0.971	1.05	
					3.50	1.06	

[a] The tetrahedral KNF model. [b] The dimer of dimer model.

the best (Figure 2C,D), although a slightly better fitting seems to be observed for the KNF model. Similar plots were also obtained for the Nbr^8AD^+ (data not shown). The most general model fits also the data, as well as the tetrahedral KNF model. On the other hand, the square KNF model cannot be excluded, since its constraints are included in the tetrahedral model. However, the tetrahedral KNF model should still be prefered because it has less free parameters. Note also from Table II that a greater number of free parameters does not automatically lead to a better fit. This shows that the underlying model, more than the number of free parameters, is the next important factor for the fitting (in the program, the effect of a larger number of free parameters is taken into account anyway by statistical means).

Table III shows a significant difference of activity among the different binding site concentrations for both ligands. This effect, and particularly the loss of binding capability below 0.3 μM, could be due to a dissociation of the protein into less active dimers. This finding is in contrast with the view of Ovadi et al. (1979) for glyceraldehyde-3-phosphate dehydrogenase from rabbit muscle. On the basis of steady-state data, these authors argue, in fact, that the enzyme is more active at lower concentration. It is difficult at the present time to reconcile the two views, other than by saying that the presence of substrate [as in the steady-state kinetic data of Ovadi and al. (1979)] may stabilize the oligomer and possibly reverse the trend observed with coenzyme alone.

The decrease of the maximal quenching for progressive binding steps is very significant. This was also observed by Schlessinger & Levitzki (1974) on rabbit muscle glyceraldehyde-3-phosphate dehydrogenase by titration at high enzyme concentration.

Discussion

The present results obtained with a new method of calculation based on a direct fitting of the protein fluorescence intensity suggest that the dimer of dimer model and the tetrahedral KNF model can both be applied to glyceraldehyde-3-phosphate dehydrogenase from sturgeon for explaining the negative cooperativity observed upon coenzyme binding, although two additional assumptions should be done (nonidentical maximal fluorescence quenchings within the oligomer and a concentration-dependent activity). Recently, Henis & Levitzki (1980b), using a new approach based on ligand competition experiments, have suggested that the mechanism of negative cooperativity of coenzyme binding to rabbit muscle glyceraldehyde-3-phosphate dehydrogenase involves successive sequential conformational changes. These latter results support our present conclusion that the tetrahedral KNF model can also be applied to glyceraldehyde-3-phosphate dehydrogenase from sturgeon. However, an induced-fit model is rather in contradiction with the generally accepted dimer of dimer structure for sturgeon glyceraldehyde-3-phosphate dehydrogenase. The latter was born out of the studies of Malhotra & Bernhard (1968, 1973). Indeed, these authors have shown that a "half-site" reagent such as furyl acryloyl phosphate is capable of reacting with fully tetrameric glyceraldehyde-3-phosphate dehydrogenase to give a difuroyl acryloyl enzyme tetramer. From these results, they concluded in favor of a dimer of dimer structure and raised the possibility of preexisting asymmetry in the tetrameric apoenzyme. The dimer of dimer structure assumption has received supports from the studies of Kelemen et al. (1975), who have interpreted their fluorescence quenching data upon NAD^+ binding in terms of two classes of independent binding sites, each with a distinct affinity. However, they seemed to not have tried to fit their data with other models such as, for instance, the KNF model.

In contrast to these experiments favoring a dimer of dimer structure model, one should remark that alkylating reagents such as iodoacetic acid, or iodoacetamide, and reversible reagents such as 5,5′-dithiobis(2-nitrobenzoate) have been shown to react at a similar rate with all four sites in glyceraldehyde-3-phosphate dehydrogenase from muscle (Levitzki,

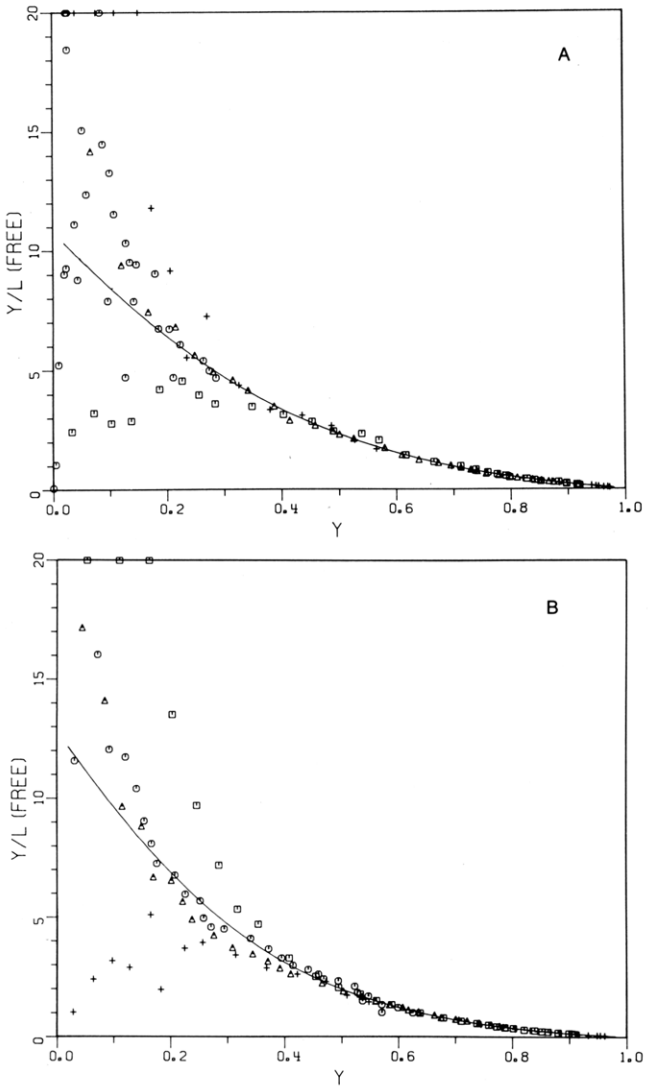

FIGURE 1: Scatchard plots. Binding saturation y and free ligand concentration L are calculated as $y(\text{measd}) = y(\text{calcd})\Delta f(\text{measd})/\Delta f(\text{calcd})$ and $L(\text{measd}) = L_{tot} - y(\text{measd})\text{act}B_{tot}$. $y(\text{calcd})$ and $f(\text{calcd})$ are calculated from the best fitting K'_i, $\Delta f_{max,i}$, and act and from L_{tot} and B_{tot}. $y(\text{measd})$ is not exactly correct with this equation because there is no linear relationship between y and Δf for different $\Delta f_{max,i}$ (but it is a good approximation). (A) NAD^+: B_{tot}, (○) 0.082 μM, (△) 0.281 μM, (□) 0.980 μM, (+) 3.570 μM. (B) Nbr^8AD^+: B_{tot}, (○) 0.082 μM, (△) 0.282 μM, (□) 0.971 μM, (+) 3.500 μM. The full lines are the computed binding curves obtained on the basis of the best fitting parameters. Note: These Scatchard plots have *not* been used to reach the conclusions, stated in this paper, about the cooperativity features of the enzyme. Our conclusions (Table II) are based on a original computational procedure (see Methods).

1974; Seydoux & Bernhard, 1974). Thus, it appears that the structure of the alkylating reagent plays an essential role in inducing (or revealing) the type of cooperativity in glyceraldehyde-3-phosphate dehydrogenase.

In the case of NAD^+, where the negative cooperativity is soundly assessed, one may raise the question as to which part(s) of the dinucleotide is (are) more responsible for the triggering of the cooperative subunit interaction. As suggested by the crystallographic data of Moras et al. (1975) and Olsen et al. (1976), the structure of the adenine part of the coenzyme seems to be the essential factor. Furthermore, Moras et al. (1975) have claimed that the adenine part of bound NAD^+ does not have the same conformation in all four subunits: in two subunits, the conformation of the adenine ring about the glycosidic bond would be anti with a $C_{2'}$ endo conformation for the ribose ring and would probably be syn with a $C_{3'}$ endo conformation in the two other subunits. By contrast, Olsen et al. (1976) have shown that Nbr^8AD^+ [2] is bound in an anti conformation to all four subunits. Our present results indicate that the binding of Nbr^8AD^+ to glyceraldehyde-3-phosphate dehydrogenase proceeds in a negative cooperative manner similar to that observed with NAD^+. This may be taken as an indication that the two coenzymes are bound in a similar manner,[3] which in turn, in contrast to the view presented by Moras et al. (1975), suggests that the negative cooperativity in NAD^+ binding is not a consequence of the structure of the adenine part.[4] This finding is in accord with the recent results of Henis & Levitzki (1980b) and Henis et al. (1979). These authors have shown that the occurrence of negative cooperative coenzyme interactions is dependent on the structure of the pyridinium part of the coenzyme. In fact, the pyridinium part of the coenzyme could play a structural role in orienting the adenine part of the coenzyme.

Another finding supports this view: an affinity label, 3-(chloroacetyl)pyridine adenine dinucleotide was recently shown to bind to glyceraldehyde-3-phosphate dehydrogenase in a noncooperative manner (for the noncovalent binary complex) (Branlant et al., 1982). Nevertheless, a clear-cut answer about the origin of the cooperativity remains a matter of debate.

A question of different nature pertains to the mechanism of protein fluorescence quenching. Energy transfer and/or conformational changes can be the cause of the different fluorescence behavior of the four binding steps. If one now takes the problem from the point of view of the detailed enzyme structure, consider that three tryptophanyl residues per subunit are present in glyceraldehyde-3-phosphate dehydrogenase from sturgeon muscle (Kelemen et al., 1975; G. Branlant et al., unpublished results) and precisely at positions 84, 193, and 310.[5] If one assumes a three-dimensional structure of sturgeon glyceraldehyde-3-phosphate dehydrogenase similar to that of the lobster and *B. stearothermophilus* enzymes, Trp-84 should be located in the interior of the protein, not far from the adenine pocket. Trp-310 would

[2] Michaelis constants (K_M) of NAD^+ and Nbr^8AD^+ for sturgeon glyceraldehyde-3-phosphate dehydrogenase were determined by Lineweaver–Burk double-reciprocal plots. Enzymic tests were done according to Ferdinand (1964). Relative value of velocity (rel V) is the percentage of that obtained with NAD^+: NAD^+, K_M = 20 μM, rel V = 100%; Nbr^8AD^+, K_M = 24 μM, rel V = 30%.

[3] If one assumes a similar binding of the adenosine moiety of NAD^+ and Nbr^8AD^+ to glyceraldehyde-3-phosphate dehydrogenase as that for liver alcohol dehydrogenase, this implies an anti conformation of the adenine ring of NAD^+ and Nbr^8AD^+ about the glycosidic bond with a $C_{2'}$ endo conformation for the ribose ring. Indeed, the refined structure of liver alcohol dehydrogenase has shown such a conformation for NAD^+ (Eklund et al., 1981). A graphic construction on display of the binary complex liver alcohol dehydrogenase–Nbr^8AD^+ has shown that Nbr^8AD^+ is bound to the enzyme in the same manner as NAD^+, but the ribose ring requires a slightly different puckering in order to avoid steric hindrance with the bromine atom (H. Eklund and J. P. Samama, unpublished results).

[4] This interpretation is supported by the results of Henis & Levitzki (1980b) and Deparade et al. (1981), who have shown that NAD^+ and derivatives of NAD^+ spin-labeled on the adenine part bind to glyceraldehyde-3-phosphate dehydrogenase from rabbit muscle and sturgeon muscle, respectively, in a negative cooperative manner. More surprisingly is the result of Pfenninger reported by Malhotra et al. (1981), which indicates that NAD^+ binds noncooperatively to glyceraldehyde-3-phosphate dehydrogenase from fish muscle.

[5] Tryptophan-84 and -310 are invariant in all known primary structures of glyceraldehyde-3-phosphate dehydrogenase (Hocking & Harris, 1980; Nowak et al., 1981). The position of the third could be 193 or 315. Pig muscle and sturgeon muscle glyceraldehyde-3-phosphate dehydrogenases have great similarities in amino acid composition and tryptic peptides (D. Tritsch, unpublished results). These results suggest that the third tryptophanyl residue is at position 193.

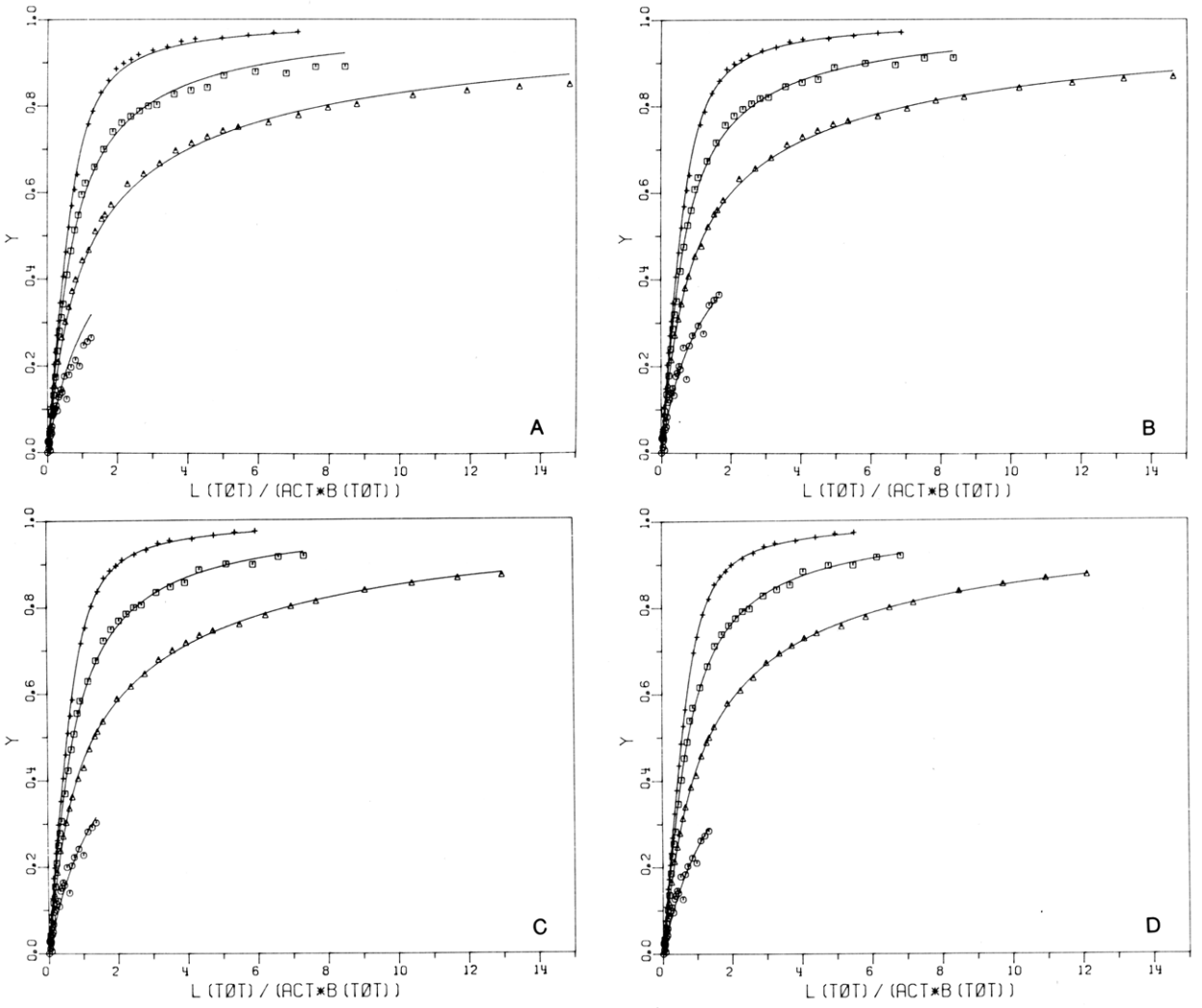

FIGURE 2: Direct plots for NAD^+ binding on glyceraldehyde-3-phosphate dehydrogenase: B_{tot}, (○) 0.082 μM, (△) 0.281 μM, (□) 0.980 μM, (+) 3.570 μM. For the lowest enzyme concentration, we only determined the data showing the first binding step. This step is less easily deduced from experiments at higher enzyme concentration. The full lines are the computed binding curves obtained on the basis of the selected parameters. For abbreviations, see Figure 1 and Methods. (A) Tetrahedral KNF model with equal efficiency quenchings for the different ligand binding steps and equal activity (i.e., the binding efficiency does not vary with protein concentration). (B) Tetrahedral KNF model with equal efficiency quenchings but independent activities. (C) Dimer of dimer model with independent efficiency quenchings and independent activities. (D) Tetrahedral KNF model with independent efficiency quenchings and independent activities.

be also buried inside near the *P* axis whereas Trp-193 would be near the *R* axis and could interact with coenzyme in the adjacent subunit (Olsen et al., 1975). This latter residue, located in the S loop, showed one of the most significant changes between the apo- and the holoenzyme (Murthy et al., 1980). It is also noteworthy that modification of Trp-193 could perturb coenzyme binding (Heilmann & Pfleiderer, 1975). A study that would differentiate the contribution of each tryptophan in the protein fluorescence would give new insights in understanding the negative cooperative behavior of glyceraldehyde-3-phosphate dehydrogenase at the molecular level.

The decrease of the maximal quenching for progressive binding steps is not surprising, it is actually in keeping with an induced-fit mechanism. In fact, the cooperative conformational changes that alter the binding affinity during the progressive binding to the oligomer may just as well produce changes in the fluorescence quantum yield. Instead of being due to conformational changes, the difference in Δf_{max} may be brought about by energy-transfer mechanisms as argued, for example, for NADH binding to horse liver alcohol dehydrogenase (Iweibo, 1976) and shown on rigid models (Royer et al., 1981). It is as yet not clear, however, if, and to what extent, the fluorescence quenching due to NAD^+ binding is due to energy-transfer mechanisms. This point is discussed in a previous paper dealing with horse liver alcohol dehydrogenase (Subramanian & Ross, 1979).

In conclusion, the results of the present investigation obtained with a new approach to fitting ligand binding data and the sparce data in the literature as cited above suggest that the cooperative binding of coenzyme to sturgeon glyceraldehyde-3-phosphate dehydrogenase could also operate via an induced-fit mechanism. With concern to the dimer of dimer model usually accepted for sturgeon glyceraldehyde-3-phosphate dehydrogenase, the possibility of alternative models (i.e., KNF model) was not taken into account by other groups and checked statistically as done here.

Registry No. NAD, 53-84-9; Nbr^8AD, 52977-37-4; glyceraldehyde-3-phosphate dehydrogenase, 9001-50-7.

References

Abdallah, M. A., Biellmann, J. F., Nordström, B., & Bränden, C. I. (1975) *Eur. J. Biochem. 50*, 475–481.

Adair, G. S. (1925) *J. Biol. Chem. 63*, 529.

Allen, G., & Harris, J. I. (1975) *Biochem. J. 151*, 747–749.

Allison, W. S., & Kaplan, N. O. (1964) *J. Biol. Chem. 239*, 2140–2152.

Biesecker, G., & Wonacott, A. J. (1977) *Biochem. Soc. Trans. 5*, 647–652.

Biesecker, G., Harris, J. I., Thierry, J. C., Walker, J. E., & Wonacott, A. J. (1977) *Nature (London) 266*, 328–333.

Branlant, G., Eiler, B., Wallén, L., & Biellmann, J. F. (1982) *Eur. J. Biochem. 127*, 519–524.

Conway, H., & Koshland, D. D. (1968) *Biochemistry 7*, 4011–4023.

Cornish-Bowden, A., & Koshland, D. E., Jr. (1970) *Biochemistry 9*, 3325–3336.

Deparade, M. P., Gloggler, K., & Trommer, W. F. (1981) *Biochim. Biophys. Acta 653*, 422–433.

Draper, N. R., & Smith, H. (1966) *Applied Regression Analysis*, p 274, Wiley, New York.

Eklund, H., Samama, J. P., Wallén, L., Bränden, C. I., Åkeson, Å., & Jones, T. A. (1981) *J. Mol. Biol. 146*, 561–587.

Ferdinand, W. (1964) *Biochem. J. 92*, 578–585.

Heilmann, H. D., & Pfleiderer, G. (1975) *Biochim. Biophys. Acta 384*, 331–341.

Henis, Y. I., & Levitzki, A. (1980a) *Eur. J. Biochem. 112*, 59–73.

Henis, Y. I., & Levitzki, A. (1980b) *Proc. Natl. Acad. Sci. U.S.A. 77*, 5055–5059.

Henis, Y. I., Levitzki, A., & Gafni, A. (1979) *Eur. J. Biochem. 97*, 519–528.

Hocking, J. D., & Harris, J. I. (1980) *Eur. J. Biochem. 108*, 567–579.

Iweibo, I. (1976) *Biochim. Biophys. Acta 446*, 192–205.

Kelemen, N., Kellershohn, N., & Seydoux, F. (1975) *Eur. J. Biochem. 57*, 69–78.

Koshland, D. E., Jr., Nemethy, G., & Filmer, D. (1966) *Biochemistry 5*, 365–385.

Levitzki, A. (1974) *J. Mol. Biol. 90*, 451–458.

MacQuarrie, R. A., & Bernhard, S. A. (1971) *Biochemistry 10*, 2456–2466.

Malhotra, O. P., & Bernhard, S. A. (1968) *J. Biol. Chem. 243*, 1243–1252.

Malhotra, O. P., & Bernhard, S. A. (1973) *Proc. Natl. Acad. Sci. U.S.A. 70*, 2077–2081.

Malhotra, O. P., Bernhard, S. A., & Seydoux, F. (1981) *Biochimie 63*, 131–141.

Monod, J., Wyman, J., & Changeux, J. P. (1965) *J. Mol. Biol. 12*, 88–118.

Moras, D., Olsen, K. W., Sebasan, M. N., Buehner, M., Ford, G. C., & Rossmann, M. G. (1975) *J. Biol. Chem. 250*, 9137–9162.

Murthy, M. R. N., Garavito, R. M., Johnson, I. E., & Rossmann, M. G. (1980) *J. Mol. Biol. 138*, 859–872.

Nowak, K., Wolny, M., & Banas, T. (1981) *FEBS Lett. 134*, 143–146.

Olsen, K. W., Moras, D., & Rossmann, M. G. (1975) *J. Biol. Chem. 250*, 9313–9321.

Olsen, K. W., Garavito, R. M., Sabesan, M. N., & Rossmann, M. G. (1976) *J. Mol. Biol. 107*, 577–584.

Ovadi, J., Batke, J., Bartha, F., & Keleti, T. (1979) *Arch. Biochem. Biophys. 193*, 28–33.

Royer, J., Beugelmans-Verrier, M., & Biellmann, J. F. (1981) *Photochem. Photobiol. 34*, 667–672.

Schlessinger, J., & Levitzki, A. (1974) *J. Mol. Biol. 82*, 547–561.

Seydoux, F., & Bernhard, S. (1974) *Biophys. Chem. 1*, 161–174.

Seydoux, F., Bernhard, S. A., Pfenninger, O., Payne, M., & Malhotra, O. P. (1973) *Biochemistry 12*, 4280–4300.

Subramanian, S., & Ross, P. D. (1979) *J. Biol. Chem. 254*, 7827–7830.

Trentham, D. R. (1968) *Biochem. J. 109*, 603–612.